

Continuous wave laser celiometer with code modulation for measurements of cloud base height

K. HOLEJKO and R. NOWAK

Warsaw University of Technology
15/19 Nowowiejska Str., 00-665 Warsaw, Poland

This paper presents a CW low power celiometer designed for cloud base height measurements. The 500-mW CW IR laser of the celiometer is modulated by a pseudo noise sequence. The scattered and delayed light signal is obtained by a correlation system with output bandwidth of only 3.5 Hz. This enables to obtain the ranges of 1.2 km to the clouds and the accuracy of the order of ± 2.5 m to the solid objects. The following problems are discussed: principle of operation, device architecture, and error estimation. Some measurement results are also enclosed.

Keywords: aerosol extinction, laser rangefinders, spread spectrum systems.

1. Introduction

Lidar has been used as a research tool for many years. Conventional lidar systems, which have been employed for most published lidar work today, make use of 0.1 to 1 J class pulsed lasers. For most applications like small airfields it is essential that laser rangefinders used as the measuring devices of cloud base height be eye safe, low cost, size and complexity, as well as portable and reliable.

The approach we took was to develop a simple and reliable lidar system for low cloud base heights, which is essential for landing purposes. The basic concept of the lidar that we will describe here is a system with 500 mW CW laser modulated by a pseudo-random sequence applied as a transmitter. The receiver employs a silicon avalanche photodetector. The transmitter and the receiver are located together in one compact unit (Fig. 1). The results of measurements are transmitted via an RS 232 link to the remote digital indicator or to the computer. In the experimental



Fig.1. General view of the celiometer.

model the 810 nm 0.5 W CW laser has been employed, so the eye safe power density of 0.5 mW/cm² occurs at a distance of 50 m from the device.

2. Celimeter structure

The basic diagram of the celimeter structure and signal processing are shown in Fig. 2. CW laser is modulated by a pseudo-random sequence generated in Shift register 1. The sequence which is 2047 bit long and has a bit length of $T_b = 266.8$ ns is additionally modulated by an auxiliary 500 Hz square wave signal. Such signal (Fig. 2b) sent to the target, like a cloud, is backscattered and delayed depending on the distance h_b , then received by the receiving

telescope. The returned signal detected by an avalanche photodetector is amplified and mixed with a locally delayed the same sequence, which modulates the laser. The delayed sequence is produced by Shift register 2 which has the same structure as Register 1, but is reseted in the predetermined state of the transmitted sequence. The locally mutual delay between sequences τ_k (Fig. 2c) is introduced slowly starting from zero up to maximal range which has been chosen as 1270 or 2550 m. As a result of the mutual sequence mixing an autocorrelation function appears at the output of the filter (Fig. 2d). The peak of the autocorrelation function appears when the locally introduced delay of the sequence equates with the delay caused by the measured distance.

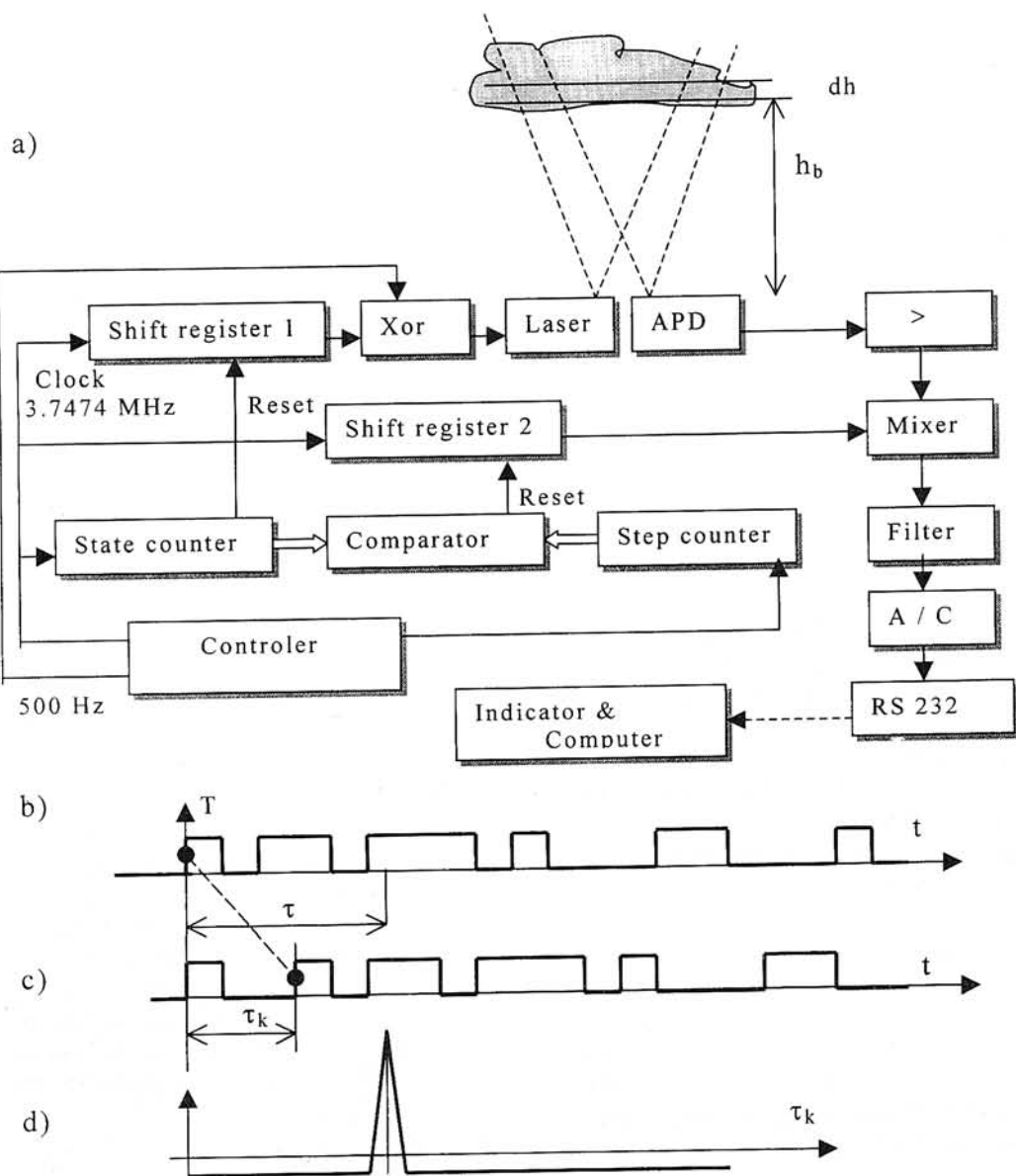


Fig.2. Celimeter structure.

The programmed delay is obtained by comparing the state of the Shift register 1 which is controlled by the State counter with the additional Step counter which can be driven in any way and speed. In our model the Step counter is filled after 127 or 255 steps each $\tau_s = 70$ ms long. So, the actual range 1270 m or 2550 m is sampled in 9 or 18 s. During one step the mutual delay of the registers is changed of $T_s = 66.7$ ns, or exactly $R_s = 10.000$ m in mean atmospheric conditions. In this manner one code bit $T = 4T_s$, consequently the triangle autocorrelation function which occupies two bits is sampled in 8 steps.

Since the states of the Step counter are changed slowly very narrow bandwidth of the correlator filter of $B \approx 1/4\tau_s = 3.57$ Hz has been used, which improves signal to noise ratio.

In order to facilitate the amplification of slowly varying signals additional modulation of 500 Hz has been applied causing the changes of autocorrelation function polarity. Such a signal after amplification and detection is sampled every $\tau_s = 70$ ms, A/C converted and sent, together with the number of the sample, to the remote indicator and computer for farther processing.

3. Prediction of the backscattered signal

Calculations of the backscattered signal for the modulated CW lidar are similar to the analysis of a conventional lidar. Light received by the receiving telescope with aperture A_0 is usually calculated summing up elementary intensities backscattered from the cloud layers at the distance $h_b + h$. Thus,

$$P(H) = A_0 P_0 a(h_b) \int_0^H P \left[t - \frac{2(h_b + h)}{c} \right] \frac{\beta(\pi)}{(h_b + h)^2} e^{-2\alpha H} dh, \quad (1)$$

where h is the distance in the cloud ranging from the cloud base h_b to the determined point of the cloud H , $a(h_b)$ is the atmospheric transmittance up to the cloud base, $P(t)$ is the laser beam power, α is the total extinction coefficient of the cloud, and $\beta(\pi)$ is the backscattering coefficient.

For the assumptions that laser power is a step function $P(t) = P_0 1(t)$, $h_b \gg h$, the distribution of aerosols in the cloud is homogenous, one can obtain the shape of the signal appearing at the receiving telescope after the delay $\tau = 2h_b/c$

$$P(H) = \frac{A_0 P_0 a(h_b) \beta(\pi)}{h_b^2} (1 - e^{-2\alpha H}). \quad (2)$$

It can be seen from Eq. (2) that the power from the cloud increases with time $t = 2H/c$ in an exponential manner while the laser beam penetrates the cloud. The power reaches its maximum at $2\alpha H > 2.3$ and it can be expressed simply as

$$P_{\max} = \frac{A_0 P_0 a(h_b) \beta(\pi)}{2h_b^2} \alpha \quad (3)$$

In Eq. (3), the influence of the cloud is expressed by the ratio of backscattering coefficient to extinction coefficient k which is a constant depended on the cloud. Different values are given for this ratio. For instance, $k = \beta(\pi)/\alpha = 0.012$ sr^{-1} [9], $k = 0.033$ sr^{-1} [11] and for cirrus $k = 0.1$ sr^{-1} [11]. Besides, the extinction coefficient is simply expressed by means of standard visibility V_n . For near IR radiation that relationship is independent of wavelength and aerosol composition like heavy fog, clouds, rain, and snow having the form [7,8]

$$\alpha = 3/V_n \text{ (km}^{-1}\text{)}. \quad (4)$$

Finally, we may summarise the results of the above analysis for the following cases:

- Laser pulses are sufficiently long comparing to the visibility in the cloud.

This case occurs for $2\alpha H > 2.3$ or $H = 1/2\tau c > 0.38 V_n$, thus, Eq. (3) should be applied

$$P_{\max} = \frac{A_0 P_0 a(h_b) \beta(\pi)}{2h_b^2} \frac{\beta(\pi)}{\alpha} = \frac{A_0 P_0 a(h_b) k}{2h_b^2}. \quad (5)$$

For the parameters used in our model $P_0 = 0.5$ W, $a(h_b) \approx 0.5$, $A_0 = 0.01$ m^2 , $k \approx 0.012$ sr^{-1} , $h = 1000$ m one can obtain $P_{\max} = 15$ pW.

- Laser pulses are short comparing to the visibility in the cloud.
- Cloud layer is very narrow.

In both cases Eq. (2) must be used that gives $P(H) < P_{\max}$.

$$P(H) = \frac{A_0 P_0 a(h_b) \beta(\pi)}{h_b^2} \frac{\beta(\pi)}{2\alpha} (1 - e^{-2\alpha H}) = \frac{A_0 P_0 a(h_b) k}{2h_b^2} \left(1 - e^{-\frac{6H}{V_n}} \right). \quad (6)$$

4. Accuracy estimation

The autocorrelation function obtained during correlation of the received and local codes has symmetrical, triangle shape having the width of two codes bits at the base. For such deterministic and symmetrical shape even two samples within the area of the triangle are sufficient to determine the position of the autocorrelation peak, which is the measure of the unknown distance. In real situations, however the shape, of the autocorrelation function changes due to signal distortions and the presence of noise.

Signal distortions

The signal distortions are caused by limited bandwidth of the input amplifier and correlator filter. As the result the autocorrelation peak is delayed and decreased. The

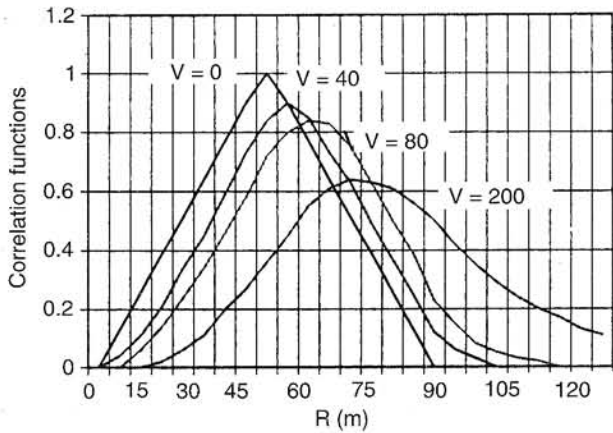


Fig.3. Distortions of the autocorrelation function.

spread-backscattered objects like clouds cause similar distortions, since, according to Eq. (1), the output signal is an integral of reflections from elementary scattering layers. Thus, the resulting autocorrelation function may be treated as an integral of elementary correlations.

In Fig. 3, some examples of autocorrelation functions obtained from clouds with different visual ranges are shown. The triangle shape appears only for hard objects $V_n = 0$, while for spread objects like clouds the correlation peak is delayed and decreased. This behaviour of peak shift may be included in the definition of the cloud base.

Noise influence

Noise appears at the output of the filter together with the autocorrelation function causing the fluctuations of its slopes Fig. 4. In order to estimate the delay of the autocorrelation peak we have applied the algorithm of "centre of gravity" for these samples which exceed the threshold U_{tr} , usually established at the half of the autocorrelation peak

$$\tau_{cg} = \frac{\sum_1^M U_i \tau_i}{\sum_1^M U_i} = \frac{\sum_1^M (V_i + n_i) \tau_i}{\sum_1^M (V_i + n_i)} \equiv \tau_{mean} + \frac{\sum_1^M n_i (\tau_i - \tau_{mean})}{\sum_1^M V_i} \quad (7)$$

True value Noise error

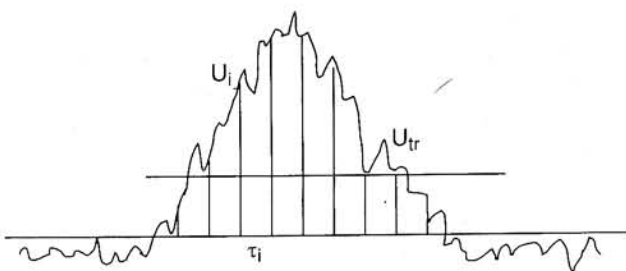


Fig.4. Influence of noise.

where U_i are the values of samples measured over the threshold U_{tr} , V_i are the real values, n_i is the noise contribution with mean equal to zero, τ_i is the steps number, τ_{mean} is the mean value of τ_{cg} with no noise presence

$$\tau_{mean} = \frac{\sum_1^M V_i \tau_i}{\sum_1^M V_i} \quad (8)$$

As it was mentioned before the autocorrelation function is sampled in 8 steps, each $\tau_s = 70$ ms long, thus sampled is the noise. Since the bandwidth of the filter is $B \approx 1/4\tau_s$ and the correlation time of the filter equals $\tau_{fil} = 1/\pi B$, thus one sample step is of the order of filter correlation time, and the noise samples can be treated as independent samples. Consequently the variance of the τ_{cg} can be treated as a sum of sample variances and may be calculated from Eq. (7)

$$\sigma_{\tau}^2 = \sigma_s^2 \frac{2 \sum_{-M/2}^{M/2} i^2}{M^2 V_{mean}^2} \sigma_n^2 = \tau_s^2 C^2 \frac{N}{S} \quad (9)$$

where C is the constant and N/S is the signal to noise ratio, similarly the standard distance error for the standard step distance R_s corresponding with τ_s is

$$\sigma_R = R_s C \sqrt{\frac{N}{S}} \quad (10)$$

For our model where the threshold is situated at the half of the correlation peak only 4 samples exceed the threshold, so $M = 4$ and $V_{mean} = 3/4 V_{max}$. In this case $C = 1.05$. Thus, if for instance $S/N = 16$, then $\sigma_{\tau} = \pm 2.65$ m.

It is necessary to mention that for strong signals the shape of the autocorrelation function is rather trapezoidal or rectangular then triangle due to limiting behaviour of the amplifiers. The variance in that case may be calculated as the quantisation variance, which is

$$\sigma_{\tau}^2 = (T_s/2)^2$$

Thus, in the model, the standard error $\sigma_{\tau} = \pm T_s/2 = \pm 33.35$ ns and $\sigma_R = \pm 5$ m.

5. Experimental results

The model is now in a state of experimental testing. Range and accuracy of the lidar were measured both to the solid objects like buildings and trees as well as range to the clouds.

Experiments have shown that the range of 1675 m to the building, covered with daub, was possible to obtain with signal to noise ratio of $S/N = 16$. Rainy clouds were also observed at the height of 950 m.

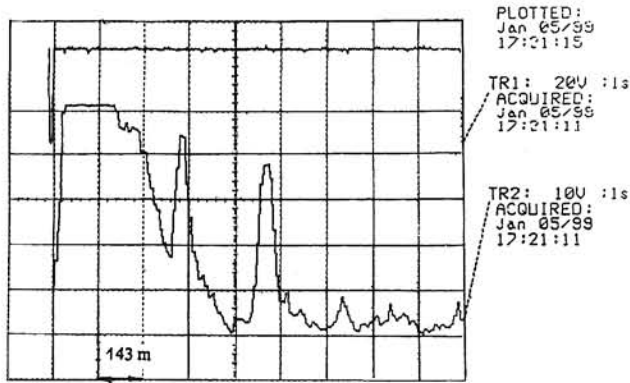


Fig.5 Correlation signal received from two clouds across the rain registered on the oscilloscope.

Performing the measurements to the remote building and changing the distance to it from 457 m to 470 m in 13 steps, each 1m long tested the accuracy of lidar. In these measurements the signal was strong and the autocorrelation function had the trapezoidal shape. The mean square error $\sigma_R = \pm 2.5$ m was obtained. Measurements were performed by means of the remote indicator, which calculates the distance according to formula (7) obtaining the data of sample values and steps number via an RS232 link.

The example of the autocorrelation function measured across the rain from two layers of clouds and registered on the oscilloscope is shown in Fig. 5. Rain and fog give strong and wide reflections at the beginning of the range, so the range gain control had to be used.

Another example of autocorrelation function measured to the green leafy tree at 1100 m was registered on the computer and shown in Fig. 6.

Acknowledgments

The laser celiometer was elaborated within the framework of the Programme „Photonics Engineering” sponsored by the Rector of Warsaw University of Technology. The work reported in this paper would not have been accomplished without the assistance of MSc Tomasz Czarnecki who elaborated the software.

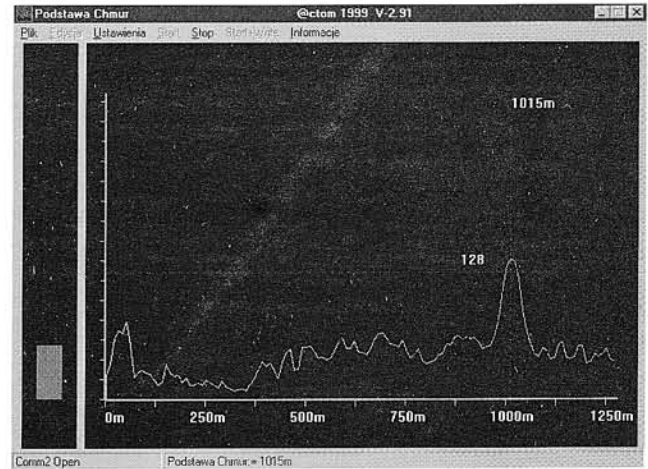


Fig.6. Correlation signal received from the green leafy tree registered on the computer.

References

1. H.N. Burns, C.G. Christodolouou, and G.D. Boreman, "System design of pulsed laser rangefinder", *Opt. Eng.* **30**, (1991).
2. R.C. Dixon, *Spread Spectrum Systems with Commercial Applications*, John Wiley & Sons, 1994.
3. C.J. Grund and E.W. Eloranta, "High spectral resolution lidar", *Opt. Eng.* **3**, 96–102, 1991.
4. M. Guasta, "Errors in the retrieval of the thin-cloud optical parameters obtained with a two boundary algorithm", *Appl. Opt.* **37**, 5522–5540 (1998).
5. K. Holejko, *Precise Electronic Measurements of Distances and Angles*, WNT, Warsaw, 1987.
6. K. Holejko, J. Siuzdak, R. Nowak, and A. Marzecki, "A multichannel short range bi-directional infrared link with code division multiple access (CDMA)", *IEEE Trans. on Consumer Electronics* **1**, (1998).
7. K. Holejko and R. Nowak, "Fog detection and visibility measurements using forward scattered radiation", *Opto-Electr. Rev.* **5**, 107–110 (1997).
8. D.L. Hutt and J.M. Theriault, "Estimating atmospheric extinction for eyesafe laser rangefinder", *Opt. Eng.* **33**, 3762–3773 (1994).
9. D.K. Kreid, "Atmospheric visibility measurement by a modulated CW lidar", *Appl. Opt.* **15**, (1976).
10. J.D. Spinhirne, "Micro pulse lidar", *IEEE Trans. on Geoscience and Remote Sensing* **31**, (1993).
11. VAISALA Aviation Weather Reporter AW11 Operators Manual, 1 February 1997.